
Estimating Relative Free Energies from a Single Ensemble: Hydration Free Energies

HEIKO SCHÄFER, WILFRED F. VAN GUNSTEREN, ALAN E. MARK

Laboratory of Physical Chemistry, Swiss Federal Institute of Technology, ETH Zentrum, CH-8092 Zürich, Switzerland

Received 9 April 1999; accepted 25 June 1999

ABSTRACT: The ability to determine the free energy of solvation for a number of small organic molecules with varying sizes and properties from the coordinate trajectory of a single simulation of a given reference state was investigated. The relative free energies were estimated from a single step perturbation using the perturbation formula. The reference state consisted of a cavity surrounded by solvent. To enhance sampling a soft-core interaction was used for the cavity. The effect of the size of the cavity, the effective core height, and the length of simulation on the ability to reproduce results obtained from thermodynamic integration calculations was considered. The results using a single step perturbation from an appropriately chosen initial state were comparable to results from thermodynamic integration calculations for a wide range of compounds. Using a large number of compounds the computational efficiency was potentially increased by 2–3 orders of magnitude over traditional free energy approaches. Factors determining the efficiency of the approach are discussed. © 1999 John Wiley & Sons, Inc. *J Comput Chem* 20: 1604–1617, 1999

Keywords: relative free energies; single ensemble; hydration free energies; solvation

Introduction

The free energy of a system is the most fundamental of all thermodynamic quantities, and methods to calculate free energies from computer

Correspondence to: W. F. van Gunsteren; e-mail: wfvgn@igc.phys.chem.ethz.ch

simulations have attracted much interest. In many fields the knowledge of relative free energies is of direct practical significance. For example, in rational drug design the binding affinity of a compound to a specific target is directly related to the free energy difference between the solvated compound and the compound–target complex. More generally, any force field used for condensed phase molecular simulations should correctly reproduce

not only properties such as the density or heat of vaporization, but also entropic properties such as solvation free energies. Unfortunately, the high cost of computing free energy differences has prohibited the widespread use of such calculations in many fields.

Calculating the absolute free energy (F) is not possible for all but the simplest of systems because it requires the knowledge of the canonical partition function Z : $F = -k_{\text{B}}T \ln Z$, where k_{B} is the Boltzmann constant and T is the temperature. Nevertheless, there is a wealth of methods¹ that can be used to calculate *relative* free energies, which are free energy differences between two states, from computer simulations. All of these methods are based on one of two fundamental approaches: the difference in free energy is determined from either the work required to transform the system from one state into another or the relative probabilities of finding the system in either of the two states.

The most general approach to estimate free energy differences, *thermodynamic integration* [TI, see eq. (2)]² belongs to the first category. Two states are connected by an arbitrary coupling parameter λ , and the work required to force the system to go from one state to the other via a reversible path is determined. TI is highly reliable, but the approach is very computationally intensive because it requires that equilibrium simulations be performed at a series of intermediate states. To scan large numbers of compounds in computer-aided drug design or to test various sets of parameters in force field development is not viable with this technique.

Therefore, many approaches^{3–11} have been proposed to reduce the required computer time by avoiding the simulation of uninteresting intermediate states. These simplifications fall roughly into three categories. Either they expand the free energy difference in a power series,^{6,8} assume a distribution for the interactions,^{3–5,7} or try to extrapolate from a reference system in a single step using the perturbation formula.¹⁰

Smith and van Gunsteren⁶ and Hummer and Szabo⁸ both expanded the free energy difference between two states in a Taylor series in the coupling parameter λ . Although the convergence of higher order terms is slow, good results were reported for changes $\leq 0.25e$ in partial charges. However, the method fails in the case of a particle being created or deleted.

King and Barford⁴ estimated the electrostatic free energy difference using linear response theory. This is equivalent to assuming the electro-

static interaction energy between a solute and the solvent to be Gaussian distributed. The results for charging a solute molecule, ranging from a sodium ion to acetic acid, were accurate within 8 kJ/mol. This method was extended by Åqvist et al.⁵ to the estimation of binding affinities. They assumed a linear response for *both* the electrostatic and the Lennard–Jones interactions and introduced a fitting parameter to scale the contribution of the Lennard–Jones interactions in order to obtain agreement with the experiment. Carlson and Jorgensen⁷ applied a similar method to the estimation of hydration free energies. However, they added an additional cavity formation term and empirically scaled the terms for electrostatic and Lennard–Jones interactions to obtain agreement with the experiment within 6 kJ/mol.

The need to introduce fitting parameters when using linear response theory suggests that the underlying assumptions do not hold. To assume that a system responds linearly to changes in the Hamiltonian is equivalent to assuming that the change in the interactions is Gaussian distributed. This approximation appears quite reasonable for changes in a uniform dielectric such as was investigated by King and Barford.⁴ However, in cases where changes in van der Waals interactions or specific hydrogen bonding interactions dominate, the approximation no longer holds. For example, in the case of water this assumption is weak. The Onsager theory¹² also assumes a Gaussian distribution when treating the solvent as a continuum and fails for water for precisely this reason.^{13,14}

Liu et al.⁹ recently reported a method that uses a single simulation at a judiciously chosen reference state and a single step extrapolation to estimate the free energy difference. The method was used to create and delete substituents on a phenol ring and used a so-called *soft-core interaction* to eliminate numerical instabilities. The results were accurate within 4 kJ/mol.

In this article we build on the work of Liu et al.⁹ by using this method to predict hydration free energies for a range of solutes from a single simulation of a reference state.

Method

Statistical mechanics identifies the free energy of a system (F) as the thermodynamic potential of the canonical ensemble $F = -k_{\text{B}}T \ln Z$, where Z is the canonical partition function. The canonical

partition function is an integral over the whole phase space (i.e., all possible momenta \mathbf{p}^N and positions \mathbf{r}^N):

$$Z = \frac{1}{N!h^{3N}} \int d\mathbf{r}^N d\mathbf{p}^N \exp\left(-\frac{\mathcal{H}(\mathbf{r}^N, \mathbf{p}^N)}{k_B T}\right), \quad (1)$$

where $\mathcal{H}(\mathbf{r}^N, \mathbf{p}^N)$ is the Hamiltonian of the system, h is Planck's constant, and N is the number of particles.

To calculate the difference in free energy between two states A and B of a system the Hamiltonian of the system \mathcal{H} may be made a function of an arbitrary coupling parameter λ . Using TI the free energy difference is evaluated as²

$$\begin{aligned} \Delta F_{BA} &= F_B - F_A = \int_{\lambda_A}^{\lambda_B} d\lambda \frac{\partial F(\lambda)}{\partial \lambda} \\ &= \int_{\lambda_A}^{\lambda_B} d\lambda \left\langle \frac{\partial \mathcal{H}}{\partial \lambda} \right\rangle_{\lambda}, \end{aligned} \quad (2)$$

where at λ_A we recover state A and at λ_B we arrive at state B . The integration in eq. (2) can be performed continuously while slowly changing the coupling parameter λ from λ_A to λ_B during the simulation. However, this approach is problematic because the system lags behind the changing Hamiltonian.^{15,16} A more controlled approach is to simulate the system at a number of fixed λ points and to evaluate the integral (2) numerically. In this way the convergence of the simulations at each λ point can be controlled and additional points (simulations) added as required.

An alternative to TI is the so-called *perturbation formula*,¹⁰ which is also based on the coupling parameter approach. The perturbation formula

$$\Delta F_{BA} = -k_B T \ln \langle e^{-(\mathcal{H}_B - \mathcal{H}_A)/k_B T} \rangle_A \quad (3)$$

estimates the free energy from the relative probability of the system in either of the two states and is exact in the sense that it does not contain any approximations. The ensemble average however holds only in the thermodynamic limit. In finite sampling the ensemble average only converges to the appropriate answer if configurations in state A are sampled that have a high probability in state B . The end state (B) must therefore not be too different from the reference state (A).

REFERENCE STATE

To use eq. (3) in the calculation of hydration free energies from a *single* simulation of a reference state it is necessary that the reference state is relevant for the pure solvent, as well as for a solvated molecule. When choosing the pure bulk solvent as the reference state (as in *Widom particle insertion*¹⁷) the probability of finding large cavities is minimal. By choosing a hard sphere cavity as the reference state no configurations representing the bulk solvent are sampled. A reference state that is suitable for the extrapolation of hydration free energies must be a compromise between the two.

The reference state used in this work consisted of a cavity with a soft-core interaction⁹ surrounded by water. The soft-core interaction is a modified Lennard-Jones interaction where the singularity $\lim_{r \rightarrow 0} V(r) = \infty$ is substituted by a core of finite height:

$$V(r; \lambda, \alpha) = (1 - \lambda)V_A(r; (1 - \lambda), \alpha) + \lambda V_B(r; \lambda, \alpha), \quad (4)$$

$$V_X(r; \lambda, \alpha) = \frac{1}{\alpha \lambda^2 C_{126}^X + r^6} \times \left(\frac{C_{12}^X}{\alpha \lambda^2 C_{126}^X + r^6} - C_6^X \right). \quad (5)$$

Here X indicates one of the two states A and B , α controls the core height, $C_{126} = C_{12}/C_6$, and $C_{12} = 4\epsilon\sigma^{12}$ and $C_6 = 4\epsilon\sigma^6$ are the Lennard-Jones parameters for the interaction between the cavity and the water oxygen. Cavities with this potential energy function and $\alpha > 0$ will be referred to as *soft-core cavities*. For a given value of λ the parameter α determines the core height at $r = 0$:

$$V_X(r = 0; \lambda, \alpha) = 4\epsilon_X \left(\frac{1 - \lambda^2 \alpha}{\lambda^4 \alpha^2} \right). \quad (6)$$

The simulations of the reference states were performed with $\lambda = 0.5$ and different sets of C_{12} , C_6 , and α values (see Table I). Four reference states that differed only in the core height were simulated. These will be referred to as C1–C4, where C1 had a core height of 5, C2 of 7, C3 of 9, and C4 of 12.2 kJ/mol, respectively. Core heights therefore varied between 2 and 5 $k_B T$. The parameters describing the reference states are given in Table I and the corresponding potential energy functions are shown in Figure 1. In a separate simulation a

TABLE I.
Parameters for Interaction between Soft-Core Cavities and Oxygen Atoms of Water Molecules.

| Cavity | ϵ (kJ/mol) | σ (nm) | C_{12} (kJ nm ¹² /mol) | C_6 (kJ nm ⁶ /mol) | α | $V(0; 0.5, \alpha)$ (kJ/mol) |
|--------|------------------------|------------------|--|------------------------------------|----------|---------------------------------|
| C1 | 0.4 | 0.6 | 3.483×10^{-3} | 0.07465 | 1.70 | 5.09 |
| C2 | 0.4 | 0.6 | 3.483×10^{-3} | 0.07465 | 1.51 | 6.99 |
| C3 | 0.4 | 0.6 | 3.483×10^{-3} | 0.07465 | 1.368 | 9.00 |
| C4 | 0.4 | 0.6 | 3.483×10^{-3} | 0.07465 | 1.21 | 12.20 |
| C5 | 0.4 | 0.4 | 2.684×10^{-5} | 6.554×10^{-3} | 1.51 | 6.99 |

See eqs. (4)–(6).

smaller cavity ($\sigma = 0.4$ nm) called C5 was also studied.

The system consisted of a single soft-core cavity (mass = 12.011 amu) in a cubic box containing 1542 simple point charge (SPC)¹⁸ water molecules at a density of 0.988 g/mL. The bonds and bond angles of the SPC molecules were constrained using the SHAKE algorithm¹⁹ with a tolerance of 10^{-4} . To keep the system at a constant temperature of 300 K, a Berendsen thermostat²⁰ was applied using a coupling time of 0.1 ps. For the calculation of the nonbonded interactions a twin range cutoff of 0.8 and 1.4 nm was used. Interactions within the larger cutoff were updated every five steps, while within the inner cutoff interactions were updated every step. To correct for the electrostatic interaction neglected beyond the cutoff of 1.4 nm, a reaction field (RF) correction²¹ with $\epsilon_{\text{RF}} = 54.0$ was used. The time step was 2 fs.

Initially, cavities C1–C4 were simulated for 800 ps with configurations saved every 0.1 ps. These

simulations are indicated by C1_{800ps}–C4_{800ps}. Later the two more promising reference states, C2 and C3, were extended to 1500 ps, which are indicated by C2_{1500ps} and C3_{1500ps}. As a final check on convergence a 10 ns trajectory (C2_{10ns}) using the parameters of cavity C2 was produced.

All the simulations were performed with the GROMOS96 simulation package.²²

EXTRAPOLATIONS

The extrapolations were performed using the GROMOS96 program PROFEE. PROFEE reads a trajectory of configurations and calculates the energy in the reference state (*A*) and in a specified end state (*B*). Because only the difference in energy is required [see eq. (3)], only the interactions that change between the two states are calculated. This greatly reduces the CPU time required to estimate the change in free energy compared to the simulation of the reference state.

Using the thermodynamic cycle shown in Figure 2, two extrapolations are required to calculate the free energy difference between bulk water and the hydrated solute. In the first extrapolation the

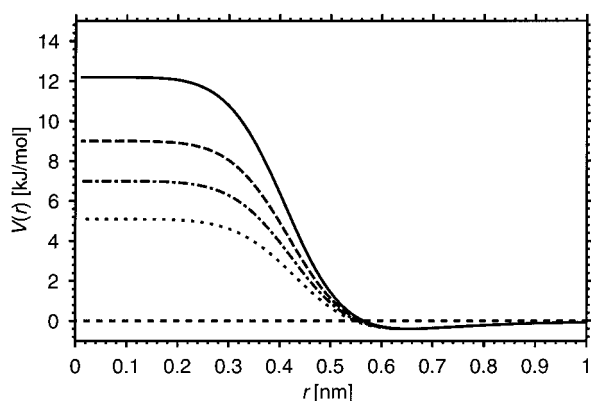


FIGURE 1. Soft-core potential energy functions $V(r; \lambda, \alpha)$ [see eqs. (4), (5)] of the reference states: (···) C1 $V(0; \lambda = 0.5; \alpha = 1.70) = 5.09$ kJ/mol, (---) C2 $V(0; 0.5, 1.51) = 6.99$ kJ/mol, (---) C3 $V(0; 0.5, 1.368) = 9.00$ kJ/mol, and (—) C4 $V(0; 0.5, 1.21) = 12.20$ kJ/mol.

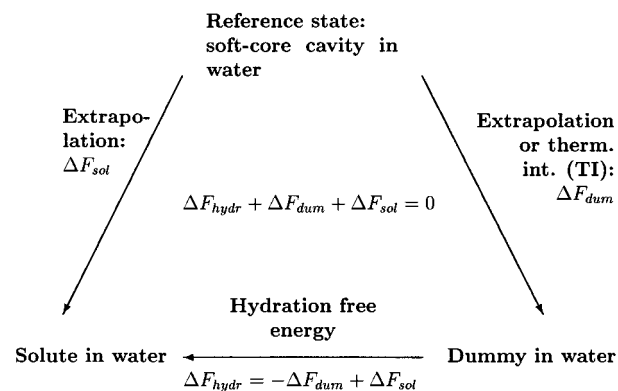


FIGURE 2. Thermodynamic cycle for calculating free energies of hydration (ΔF_{hydr}).

soft-core cavity is perturbed to a dummy cavity that does not interact with the solvent. This gives the free energy difference ΔF_{dum} between the reference state and bulk water. In the second extrapolation a *ghost* solute molecule (of a given type) is added to the reference state. The ghost molecule has no intermolecular but all intramolecular interactions. The GROMOS96²² force field (code 43A1) was used for the solute molecules. The soft-core cavity is perturbed to a dummy while the intermolecular interactions of the ghost solute with its surroundings are switched on. This results in the free energy difference between the reference state and the hydrated solute ΔF_{sol} . From Figure 2, it is clear that the free energy of hydration of the solute is

$$\Delta F_{\text{hydr}} = -\Delta F_{\text{dum}} + \Delta F_{\text{sol}}. \quad (7)$$

Results and Discussion

CHOICE OF CORE HEIGHT

Reference State

Figure 3 shows radial distribution functions between the center of the cavity and the oxygen atom of the water molecules for the four reference states C1–C4, which only differ in the core height. For the cavity with the highest core height (C4, 12 kJ/mol) the probability of finding a water molecule inside the cavity is near zero and the radial distribution function is very similar to that of a

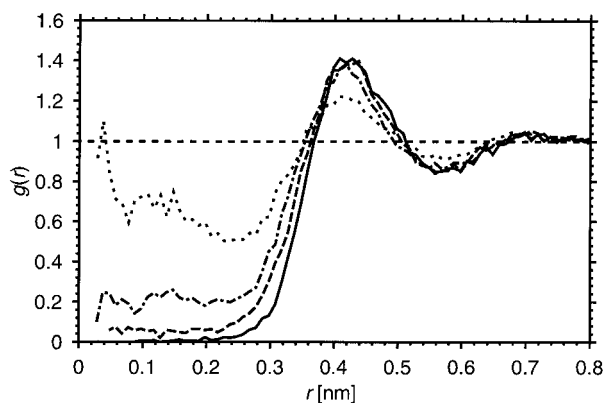


FIGURE 3. Radial distribution function between the center of the soft-core cavity and the oxygen atom of solvent water molecules obtained from a 800 ps simulation of the four reference states: (···) C1_{800ps}, (— · —) C2_{800ps}, (---) C3_{800ps}, and (—) C4_{800ps}. See also the caption of Figure 1.

Lennard–Jones particle in water. With decreasing core height (going from C4 to C1) the probability of water penetrating the cavity increases. For the cavity with the lowest core height (C1) the probability of water penetrating the cavity is roughly 60%.

Together with the increasing penetration of water, a change in the radial distribution function is observed. From simulation studies and analytical calculations on hard sphere fluids²³ it is known that the shape of the radial distribution function is primarily due to the repulsive part of the potential energy function: with decreasing core height $g(r)$ is flattened. Nevertheless, some structure is maintained, because the slope of the soft-core interaction between the minimum and the plateau region is similar to the slope of a Lennard–Jones potential energy function.

Figure 4 shows the distribution for the interaction energy between the cavity and the solvent. The only interaction is the van der Waals interaction between the cavity center and the oxygen atoms of the surrounding water molecules. The distributions are broader for cavities C2 and C3 than for C1 and C4, which are the cavities with the highest and lowest probability of water penetration, respectively. This indicates that as water penetration progresses more into the cavity the sampling of different energies at first increases, reaches a maximum with the cavity C2 [$V(r=0) \approx 7$ kJ/mol], then decreases again as the reference state becomes more similar to bulk water; 7 kJ/mol is approximately the average kinetic energy of a SPC water molecule (three rotational and three

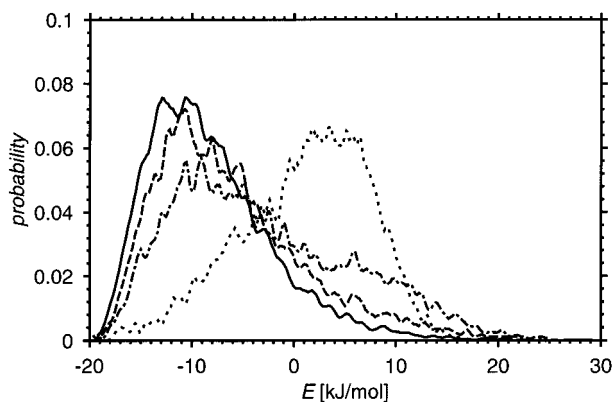


FIGURE 4. Distribution of Lennard–Jones interaction energy E between the cavity and water obtained from a 800 ps simulation of the four reference cavities: (···) C1_{800ps}, (— · —) C2_{800ps}, (---) C3_{800ps}, and (—) C4_{800ps}.

translational degrees of freedom):

$$\langle E_{\text{kin}} \rangle = 6 \times \frac{1}{2} k_B T \approx 7.5 \text{ kJ/mol.} \quad (8)$$

A broad energy distribution indicates that a wide variety of configurations is sampled in the trajectory (e.g., configurations in which the cavity is filled or unfilled). The probability of finding configurations appropriate for the greatest number of end states is therefore expected to be highest in the case of cavity C2.

Free Energy of Hard-Core Cavity Formation

The first test of the extrapolation technique consisted of reproducing the free energy of cavity formation with the extrapolations. As shown in Figure 2, two extrapolations are needed: the extrapolation to a dummy atom in water and the extrapolation to a cavity with a Lennard–Jones interaction. This end state consists of an impenetrable cavity (a *hard-core cavity*) in contrast to the soft-core cavity that is the reference state. Because all four soft-core cavities have the same Lennard–Jones parameters (Table I), the free energy of formation of the hard-core cavity must be the same for all four.

The free energy of forming a hard-core cavity was also calculated by TI. Twenty λ points were used. At each point the system was equilibrated for 10 ps and then averages were taken over the following 20 ps. The calculation yielded $\Delta F_{\text{cav}}^{\text{TI}} = 31.5 \text{ kJ/mol}$. The results for the extrapolations are summarized in Table II. As a measure of the reliability of the extrapolations the *sampling efficiency* introduced by Wood et al.²⁴ was calculated. This was an attempt by Wood and colleagues to give an estimate of the error due to finite sampling in free energy perturbation calculations by estimating to what extent important parts of the energy distribu-

tion were sampled.²⁴ The sampling efficiency S_{eff} is defined as

$$S_{\text{eff}} = 2 \frac{\text{number of configurations with } \Delta E^* \leq \Delta F^*}{\text{number of configurations}}. \quad (9)$$

The asterisks denote dimensionless energies (divided by $k_B T$). For the ideal case of a symmetric distribution of energies around $\Delta E^* = \Delta F^*$, the sampling efficiency is one. Because the sampling efficiency is a probability, the values for the single extrapolations were multiplied to give a value for the reliability of the total free energy change (ΔF_{cav}).

The free energy of cavity formation is well reproduced by extrapolations from the soft-core cavities C1_{800ps} and C2_{800ps}. The sampling efficiency can be used to judge how reliable these results are. From Table II it is obvious that the reliability of the extrapolation to the dummy atom decreases with increasing core height and this trend is reversed for the extrapolation to the hard-core cavity. Therefore, the *extreme* cases C1_{800ps} and C4_{800ps}, which have the lowest and highest core heights, respectively, fail in one of the extrapolations and their overall sampling efficiency is low. The highest overall S_{eff} is found for C2_{800ps} [$V(r=0) \approx 7 \text{ kJ/mol}$]. From the sampling efficiency one could conclude that the agreement between the results from the extrapolations and the TI calculations for C1 is simply fortuitous.

Another way to judge the convergence of the extrapolations is by looking at the time evolution of the free energy estimate. Figure 5 shows the time evolution of the free energy for the extrapolation to a dummy cavity in water. The four curves look well converged. C1_{800ps}, C2_{800ps}, and C3_{800ps} show some steps (e.g., C3_{800ps} at 100 ps). C4_{800ps}

TABLE II.
Free Energies of Cavity Formation for Hard-Core Cavity (ΔF_{cav}).

| Cavity | ΔF_{dum} (kJ/mol) | S_{eff} | ΔF_{hcc} (kJ/mol) | S_{eff} | ΔF_{cav} (kJ/mol) | S_{eff} |
|---------------------|-------------------------------------|----------------------|-------------------------------------|----------------------|-------------------------------------|----------------------|
| C1 _{800ps} | −6.5 | 0.204 | 22.9 | 5.6×10^{-3} | 29.4 | 1.1×10^{-3} |
| C2 _{800ps} | −10.6 | 0.172 | 18.8 | 0.046 | 29.4 | 7.9×10^{-3} |
| C3 _{800ps} | −11.3 | 0.026 | 15.7 | 0.039 | 27.0 | 1.0×10^{-3} |
| C4 _{800ps} | −19.5 | 2.5×10^{-3} | 13.6 | 0.7 | 33.1 | 1.8×10^{-4} |
| TI | | | | | 31.5 | |

Shown are the results for the extrapolation from the four soft-core reference cavities C1–C4 to pure water (ΔF_{dum}) and the hard-core cavity (ΔF_{hcc}) and the sampling efficiencies (S_{eff}) for both. TI, the result from thermodynamic integration.

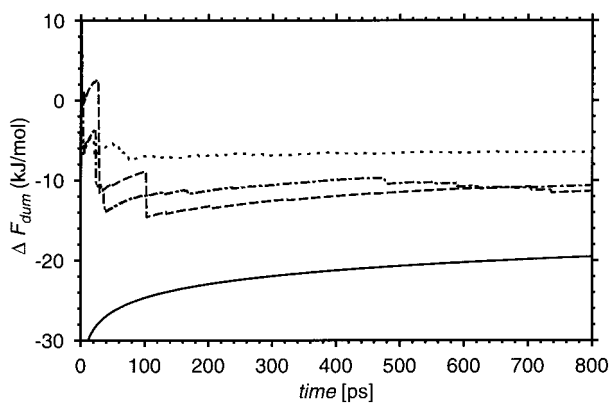


FIGURE 5. Time evolution of the free energy difference ΔF_{dum} between the soft-core cavity and a dummy cavity obtained from a 800 ps simulation of the four reference cavities: (\cdots) $C1_{800\text{ps}}$, ($-\cdot-$) $C2_{800\text{ps}}$, ($---$) $C3_{800\text{ps}}$, and ($—$) $C4_{800\text{ps}}$.

appears very smooth with a single step. These steps correspond to the sampling of configurations that are very probable in the end state that sharply lower the free energy. An absence of large steps indicates that either the configurations sampled in the reference state are not important for the end state in which case the extrapolation converges to a wrong result or all configurations have equally high probability in the end state. The curves in Figure 5 confirm the trend indicated by the sampling efficiency for the extrapolation to a dummy in water: with increasing core height the results are less reliable. The equivalent of Figure 5 for the extrapolation from the soft-core cavities to the hard-core cavity looks much the same as Figure 5, but the best sampling efficiency is for soft-core cavity C4. However, we note that the sampling efficiency S_{eff} is just a rough guide at best. As with all other such estimates it suffers from the fact that if one has not sampled a representative and uncorrelated collection of configurations one cannot pre-

dict the effect of the configurations that have not yet been sampled: all perturbation approaches suffer from a lack of unambiguous convergence criteria.

Free Energy of Soft-Core Cavity Formation

To have a more direct comparison between TI calculations and the extrapolations, TI calculations for the free energy of soft-core cavity formation were performed. The results were compared to those of the single extrapolation between the soft-core reference state and a dummy cavity in water. The TI calculations were initially performed using 20 equally spaced λ points and the system was equilibrated for 20 ps at each point with 50 ps sampling. For the cavities C2, C3, and C4 additional λ points were inserted at places where the derivative of the free energy to λ ($\partial F/\partial\lambda$) changed rapidly.

In this calculation the four cavities will yield different results. The accuracy of the extrapolation is expected to increase with decreasing core height, because the reference state becomes more similar to pure water. The profile for the TI is shown in Figure 6. The results are summarized and compared to those of the extrapolations in Table III. The trends that were anticipated are confirmed by the data: the biggest discrepancy between extrapolation and TI shows up for the cavities with a low penetration of water (C4 and C3). The very low error for C2 is fortuitous.

From the tests described above it is clear that the cavities with the lowest (C1) and highest (C4) core height are not appropriate for our purposes. The cavity (C1) with a high probability of water penetration fails in the extrapolation to a hydrated solute. An overlap between the solute molecule and one or more water molecules occurs in each configuration. The cavity with the highest core

TABLE III. Free Energy of Cavity Formation of Soft-Core Cavity (ΔF_{scc}) Obtained by Extrapolation and Results from TI Calculations.

| Cavity | 800 ps | | | 1500 ps | |
|--------|---|---|------------------------------|---|------------------------------|
| | $\Delta F_{\text{scc}}^{\text{TI}}$ (kJ/mol) | $\Delta F_{\text{scc}}^{\text{extrap}}$ (kJ/mol) | $\Delta\Delta F$ (kJ/mol) | $\Delta F_{\text{scc}}^{\text{extrap}}$ (kJ/mol) | $\Delta\Delta F$ (kJ/mol) |
| C1 | -5.6 | -6.5 | 0.9 | — | — |
| C2 | -10.9 | -10.6 | 0.3 | -10.8 | 0.1 |
| C3 | -13.9 | -11.3 | 2.6 | -11.6 | 2.3 |
| C4 | -16.8 | -19.5 | 2.8 | — | — |

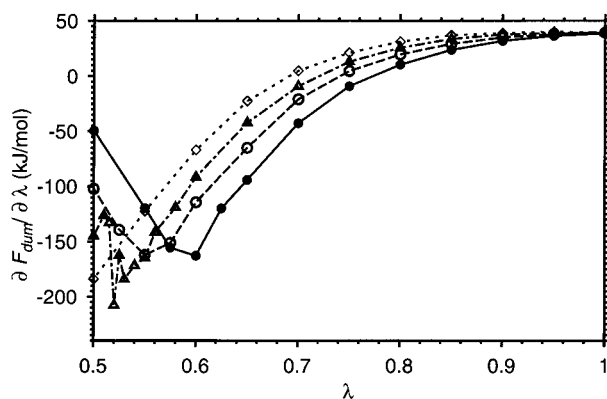


FIGURE 6. Multiple window thermodynamic integration ($\Delta F_{\text{dum}}^{\text{TI}}$) from the soft-core cavity ($\lambda = 0.5$) to pure water ($\lambda = 1.0$): (\diamond) C1, (Δ) C2, (\circ) C3, and (\bullet) C4.

height (C4) is effectively equivalent to a hard-core cavity and only rarely are configurations found that are appropriate for pure water. In addition, for a small hydrated solute few water molecules are near enough to accurately represent the first hydration shell.

HYDRATION FREE ENERGIES

Having established an appropriate range of core heights, the simulations of cavities C2 and C3 were extended to 1500 ps. With these extended trajectories, referred to as $C2_{1500\text{ps}}$ and $C3_{1500\text{ps}}$, respectively, hydration free energies of a wide range of compounds were calculated. As shown in Figure 2, an extrapolation from the reference state (soft-core cavity) to the compound in the cavity is necessary for each compound. The extrapolation from the reference state to a dummy in water is

only calculated once for each reference state (cavities $C2_{1500\text{ps}}$ and $C3_{1500\text{ps}}$).

The end states (compounds) consisted of hydrated methane (CH_4), propane, butane, isobutane, pentane, cyclopentane, carbon tetrachloride (CCl_4), chloroform (CHCl_3), water (H_2O), methanol, and ethanol.

The results from the free energy extrapolations are compared to data that were calculated using TI rather than to experimental data in order to address methodological rather than force field questions. Nevertheless, where available, the experimental data are given. The results are summarized in Tables IV–VI.

Convergence

In Table IV the results from trajectories of different length, $C2_{800\text{ps}}$ and $C2_{1500\text{ps}}$, are compared with the hydration free energies from TI. While some improvement is observed for methane, propane, methanol, and ethanol, the results for all other compounds are unchanged or less accurate.

Because there is no variational principle in the perturbation formula it is hard to judge if the amount of phase space sampled was sufficient. Very rare favorable configurations can drastically lower the free energy, even if the results seem converged (according to the sampling efficiency or number and height of jumps in ΔF as a function of simulation time). For this reason a 10 ns trajectory for the reference state C2 was generated using a different starting configuration and is therefore statistically completely independent of $C2_{800\text{ps}}$ and $C2_{1500\text{ps}}$. The results are summarized under the label $C2_{10\text{ns}}$ in Table IV. No clear trend emerges:

TABLE IV. Effect of Trajectory Length on Hydration Free Energies (ΔF_{hydr}) Extrapolated from Cavity C2.

| Compound | ΔF_{hydr} (kJ/mol) | | | | |
|----------------------|-----------------------------------|----------------------|--------------------|-------|--------|
| | $C2_{800\text{ps}}$ | $C2_{1500\text{ps}}$ | $C2_{10\text{ns}}$ | TI | Exp. |
| CH_4 | 6.7 | 7.2 | 7.5 | 8.0 | 8.37 |
| Propane | 7.2 | 9.4 | 7.7 | 9.0 | 8.18 |
| Butane | 9.9 | 10.6 | 9.1 | 7.7 | 8.70 |
| Isobutane | 10.4 | 10.4 | 6.9 | 10.5 | 9.70 |
| Pentane | 13.7 | 15.5 | 12.4 | 13.8 | 9.76 |
| CHCl_3 | 3.2 | 3.3 | 1.8 | -0.7 | -4.46 |
| H_2O | -16.9 | -16.8 | -19.3 | -24.3 | -24.02 |
| Methanol | -4.3 | -12.9 | -9.9 | -20.8 | -21.40 |
| Ethanol | -4.1 | -7.6 | -4.5 | -14.2 | -20.98 |

TI, the thermodynamic integration results.

TABLE V.
Dipole Moment (μ) and Extrapolated Hydration Free Energies ($\Delta F_{\text{hydr}}^{\text{extrap}}$) of Solutes.

| Compound | μ (D) | ΔF_{hydr} (kJ/mol) | | | | Exp. |
|-------------------|-----------|-----------------------------------|----------------------|---------------------|-------|--------|
| | | C2 _{1500ps} | C3 _{1500ps} | C5 _{880ps} | TI | |
| CH ₄ | 0.0 | 7.2 | 5.1 | 7.2 | 8.0 | 8.37 |
| Propane | 0.0 | 9.4 | 7.0 | 9.9 | 9.0 | 8.18 |
| Butane | 0.0 | 10.6 | 7.8 | 39.5 | 7.7 | 8.70 |
| Isobutane | 0.0 | 10.4 | 6.7 | 28.7 | 10.5 | 9.70 |
| Pentane | 0.0 | 15.5 | 23.3 | 270.8 | 13.8 | 9.76 |
| Cyclopentane | 0.0 | 3.8 | 2.6 | — | 7.0 | 5.02 |
| CCl ₄ | 0.0 | 1.9 | 5.4 | — | 0.4 | 0.40 |
| CHCl ₃ | 1.097 | 3.3 | 0.7 | 34.4 | -0.7 | -4.46 |
| H ₂ O | 2.260 | -16.8 | -13.5 | -15.2 | -24.3 | -24.02 |
| Methanol | 1.910 | -12.9 | -14.5 | -9.6 | -20.8 | -21.40 |
| Ethanol | 1.788 | -7.6 | -7.4 | -4.6 | -14.2 | -20.98 |

For comparison the free energies $\Delta F_{\text{hydr}}^{\text{TI}}$ calculated by thermodynamic integration (TI) are given.

methane, butane, pentane, chloroform, and water show improved estimates; propane, isobutane, methanol, and ethanol are worse compared to the TI results. Even with a 10 ns trajectory convergence is not assured, but at least for the nonpolar compounds the results lie within 4 kJ/mol of the exact TI values.

Core Height Dependence

Table V compares the results from the two extended trajectories C2_{1500ps} and C3_{1500ps} that differ only in the height of the core. For the compounds methane, propane, and isobutane we have converged results. For those compounds the results for C3_{1500ps}, the cavity with the larger core height, are consistently about 2 kJ/mol lower than the TI values. This can be explained by the poor performance of C3_{1500ps} in the extrapolation toward pure water, which is due to the low probability of finding water in the cavity C3_{1500ps} (see earlier section). The extrapolated free energy differences between the soft-core cavities and pure water are very similar for C2_{1500ps} and C3_{1500ps} (-10.8 and -11.6 kJ/mol, respectively), and the free energy of soft-core cavity formation of cavity C3_{1500ps} is less negative than expected.

Because the free energy difference between the reference cavity and the dummy cavity in water need to be calculated only once, TI can be used to determine the free energy of forming the soft-core cavity without a significant loss of efficiency. Substituting the TI values (from earlier section) for the mutation to pure water, the value for C2_{1500ps} is hardly changed. For C3_{1500ps} the free energy of

forming the soft-core cavity obtained from TI ($\Delta F_{\text{dum}}^{\text{TI}}$) is approximately 2 kJ/mol lower, thereby significantly improving the agreement of $\Delta F_{\text{hydr}}^{\text{extrap}}$ with the $\Delta F_{\text{hydr}}^{\text{TI}}$ values. In Table VI the free energy for the extrapolation to pure water has been substituted by the more accurate TI results. Both cavities yield more comparable results. The correlation between the hydration free energies obtained from the extrapolation and from TI are shown in Figure 7.

Compounds

Apart from the dependence of the results on the core heights, which could be largely eliminated by substituting one extrapolation by TI as shown above, the quality of the results differs widely for the various compounds. From Table VI it can be seen that for methane, propane, and isobutane, the results are highly accurate ($\Delta\Delta F < 1$ kJ/mol compared to TI). Results for butane and cyclopentane are reasonable ($\Delta\Delta F < 3$ kJ/mol) while for pentane, carbon tetrachloride, water, methanol, and ethanol the results are not within an acceptable range ($\Delta\Delta F > 3$ kJ/mol).

These numbers are subject to noise coming from the limited convergence (see earlier section). Nevertheless, there is a ranking in the reliability of the free energy estimates according to the number of important configurations sampled (i.e., the frequency of major jumps lowering the free energy estimate). Bulky compounds that are large compared to the size of the cavity have less reliable free energy estimates (e.g., pentane, cyclopentane, carbon tetrachloride). Because of the frequently

TABLE VI.

Hydration Free Energies of Solutes Using Extrapolation for Change from Soft-Core Cavity to Solute (ΔF_{sol}) and Thermodynamic Integration (TI) for Change from Soft-Core Cavity to Pure Water (ΔF_{dum}).

| Compound | μ (D) | ΔF_{hydr} (kJ/mol) | | | |
|-------------------|-----------|-----------------------------------|----------------------|-------|--------|
| | | C2 _{1500ps} | C3 _{1500ps} | TI | Exp. |
| CH ₄ | 0.0 | 7.2 | 7.4 | 8.0 | 8.37 |
| Propane | 0.0 | 9.4 | 9.3 | 9.0 | 8.18 |
| Butane | 0.0 | 10.6 | 10.1 | 7.7 | 8.70 |
| Isobutane | 0.0 | 10.4 | 9.0 | 10.5 | 9.70 |
| Pentane | 0.0 | 15.5 | 25.6 | 13.8 | 9.76 |
| Cyclopentane | 0.0 | 3.9 | 4.9 | 7.0 | 5.02 |
| CCl ₄ | 0.0 | 2.0 | 7.7 | 0.4 | 0.40 |
| CHCl ₃ | 1.097 | 3.3 | 3.0 | -0.7 | -4.46 |
| H ₂ O | 2.260 | -16.8 | -11.2 | -24.3 | -24.02 |
| Methanol | 1.910 | -12.9 | -12.2 | -20.8 | -21.40 |
| Ethanol | 1.788 | -7.6 | -5.1 | -14.2 | -20.98 |

See also Figure 2. For comparison the free energies $\Delta F_{\text{hydr}}^{\text{TI}}$ calculated using TI are also given.

occurring Lennard–Jones overlaps between the solute and solvent, only a few favorable configurations are sampled.

The compounds that give the best results (methane, propane, and isobutane) are all small, nonpolar, and rigid). The value for methane (Fig. 8) is well converged by 400 ps, that of propane by 600 ps, and that of butane and isobutane by about 1001 ps.

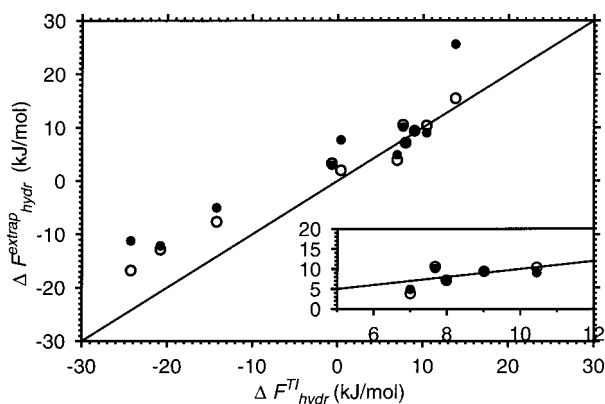


FIGURE 7. Correlation between the extrapolated hydration free energies ΔF_{hydr} (with the difference between water and the soft-core cavity calculated by TI) and free energies $\Delta F_{\text{hydr}}^{\text{TI}}$ from full TI calculations. Shown are the results from simulations (○) C2_{1500ps} and (●) C3_{1500ps} (see Table VI). (—) the ideal case of a one to one correspondence between the extrapolation and TI values.

Polar Compounds

Water, methanol, and ethanol are each small enough to fit into the cavities. In addition, from Figure 9 the estimated free energies appear reasonably converged. Nevertheless, the hydration free energies are far from the TI results. This is due to the hydrophobicity of the reference state. A polar solute in a polarizable environment will induce long-range order. There will be a correlation be-

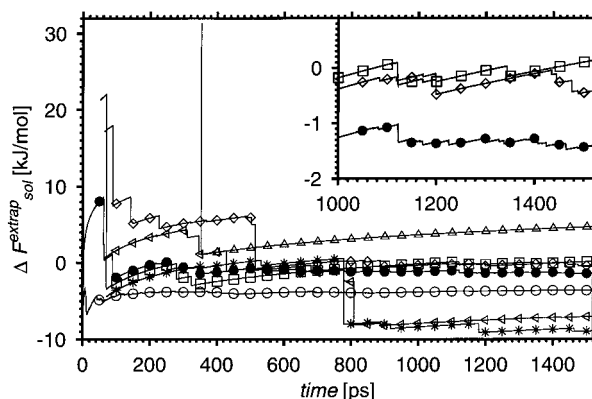


FIGURE 8. Time evolution of the extrapolated free energy difference between the soft-core reference cavity (C2) and the hydrated solute ($\Delta F_{\text{sol}}^{\text{extrap}}$) for the nonpolar solutes: (○) methane, (●) propane, (□) butane, (◇) isobutane, (△) pentane, (◁) cyclopentane, and (*) carbon tetrachloride.

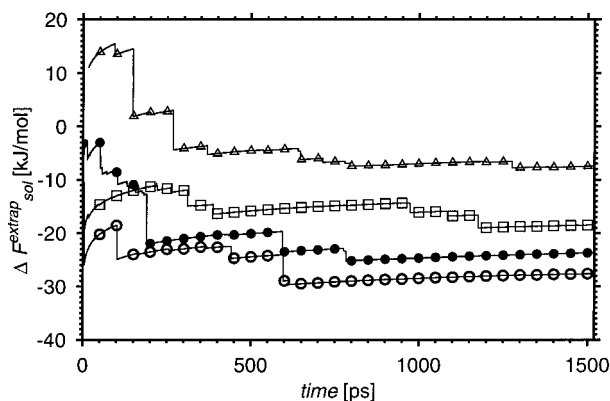


FIGURE 9. Time evolution of the extrapolated free energy difference between the soft-core reference cavity (C2) and the hydrated solute ($\Delta F_{\text{sol}}^{\text{extrap}}$) for the polar solutes: (○) water, (●) methanol, (□) ethanol, and (△) chloroform.

tween the dipole of the solute and the dipoles of the surrounding water molecules. Because the reference state is hydrophobic, there will not be any dipole–dipole correlation and thus the end state we extrapolate to is in this respect *unphysical*.

There is a low probability of sampling configurations with a long-range order appropriate for a hydrated polar solute. Such configurations will drastically lower the free energy. For example, in the extrapolation to water in the $C2_{10\text{ns}}$ reference simulation a single configuration lowered the free

energy estimate by 10 kJ/mol and this is the reason for the improvement shown in Table IV. Polar solutes therefore suffer much more from finite sampling errors than nonpolar solutes, resulting in less reliable free energy estimates.

Internal Degrees of Freedom

Although the estimate for butane is well converged, it does not reproduce the TI result. In the extrapolations only a single configuration for each solute molecule was used. Internal degrees of freedom were ignored. In the case of rather rigid molecules like propane and isobutane this approximation works well. In more flexible molecules, specifically molecules with dihedral angle degrees of freedom, such as butane, the approximation of rigidity is too crude and the contribution of the internal degrees of freedom to the free energy must be considered (see below).

CORRECTIONS FOR FLEXIBLE MOLECULES

Until now the internal energies of the solute molecules were not included: in the exponential of the perturbation formula eq. (3) the intramolecular energy contributions to the Hamiltonians cancel if we assume them to be the same in the gas phase and the hydrated phase. However, the Hamiltonian of the reference state is implicitly present in the ensemble average of eq. (3):

$$\Delta F_{B,A} = -k_B T \ln \langle e^{-(\mathcal{H}_B - \mathcal{H}_A)/k_B T} \rangle_A \quad (10)$$

$$= -k_B T \ln \frac{\int d\mathbf{r}^N d\mathbf{p}^N \exp\left(-\frac{\mathcal{H}_B - \mathcal{H}_A}{k_B T}\right) \exp(-\mathcal{H}_A/k_B T)}{\int d\mathbf{r}^N d\mathbf{p}^N \exp(-\mathcal{H}_A/k_B T)}. \quad (11)$$

The simulation of the reference state uses the Hamiltonian $\mathcal{H}_A = \mathcal{H}(\text{cavity}) + \mathcal{H}(\text{water}) + \mathcal{V}(\text{cavity-water}) + \mathcal{V}(\text{water-water})$ (i.e., only the cavity and water kinetic energy, the interactions between the soft-core cavity and the solvent, and the interactions between the solvent molecules are included). The reference state should in principle

also incorporate the solute in the gas phase (i.e., intramolecular interactions within the solute).

To correct the reference state, the configurations including the solute have to be sampled with the probability $e^{-\mathcal{H}_{\text{ref}}/k_B T}$ with

$$\mathcal{H}_{\text{ref}} = \mathcal{H}_A + \mathcal{V}_{\text{intra}}. \quad (12)$$

Here $\mathcal{V}_{\text{intra}}$ is the potential energy of the intramolecular interactions. Using this in eq. (11) yields

$$\Delta F_{BA} = -k_B T \ln \frac{\int d\mathbf{r}^N d\mathbf{p}^N \exp\left(-\frac{\mathcal{H}_B - \mathcal{H}_A}{k_B T}\right) \exp\left(-\frac{\mathcal{H}_A + \mathcal{V}_{\text{intra}}}{k_B T}\right)}{\int d\mathbf{r}^N d\mathbf{p}^N \exp(-(\mathcal{H}_A + \mathcal{V}_{\text{intra}})/k_B T)} \quad (13)$$

$$= -k_B T \ln \frac{\langle e^{-(\mathcal{H}_B - \mathcal{H}_A)/k_B T} e^{-\mathcal{V}_{\text{intra}}/k_B T} \rangle_A}{\langle e^{-\mathcal{V}_{\text{intra}}/k_B T} \rangle_A}. \quad (14)$$

Equation (14) can be understood as a form of umbrella sampling,²⁵ where the ensemble was biased by a function that exactly cancels the intramolecular interactions $\mathcal{V}_{\text{intra}}$. From eq. (14) it is clear why, when using a single solute configuration, one can ignore all internal interactions. The intramolecular interaction $\mathcal{V}_{\text{intra}}$ is independent of the coordinates, and thus $\exp(-\mathcal{V}_{\text{intra}}/k_B T)$ can be taken out of the ensemble averages in the nominator and denominator and cancel, giving eq. (11).

Correction for Butane

The correction described above was used with the extrapolation toward butane in the reference cavity C2_{1500ps}. For each configuration in the trajectory of the reference state 10 configurations of butane with a random dihedral angle value were inserted into the cavity and the free energy difference was calculated according to eq. (14). Bond angles and bond lengths of the butane molecule were kept fixed.

The result for the extrapolation from the reference state cavity C2_{1500ps} to the hydrated butane is $\Delta F_{\text{hydr}}^{\text{dih}}(\text{butane}) = -1.2$ kJ/mol. This yields a hydration free energy of 9.4 kJ/mol compared to the uncorrected value of 10.6 kJ/mol. This is certainly a better estimate. An additional contribution may also arise from the bond angle degrees of freedom. This was checked by making the bond angles vary randomly by $\pm 5^\circ$ around their equilibrium value. The corrected free energy estimate is $\Delta F_{\text{hydr}}^{\text{dih}+\text{ang}}(\text{butane}) = -1.3$ kJ/mol. This results in a slightly improved hydration free energy of 9.3 kJ/mol. The contribution of the bond angle degrees of freedom seems to be negligible.

EFFECT OF CAVITY SIZE

It is obvious that the size of the cavity must be comparable to or larger than the size of the solute.

The question arises as to what extent the results depend on the size of the cavity. In a new simulation the reference cavity (C5) with the same values for the α and λ parameters as C2 except for σ , which was decreased to 0.4 nm (Table I), was simulated. The trajectory had a length of 880 ps. The radial distribution function of simulation C5_{880ps} (not shown) was very similar to the radial distribution function of simulation C2_{800ps} (Fig. 3), except that it was shifted to smaller distances. The probability of finding water inside the cavity was the same as for cavity C2_{800ps}.

In Table V the results for the hydration free energies of C5_{880ps} are given. As expected, extrapolations involving the large solutes butane, isobutane, pentane, and CHCl₃ fail because of the smaller size of the reference cavity. For the smaller solutes, however, the quality of the results does not seem to strongly depend on the size of the cavity and the smaller cavity does not significantly improve the efficiency, except perhaps in the case of methane. Looking at the structure of the radial distribution function in Figure 3 it might be anticipated that the position of the first peak, which depends on the cavity size, would influence the efficiency of the approach for a given solute. Such size dependence seems to be weak.

TIMING

The efficiency of the presented extrapolation method stems from the drastic reduction in the number of interactions that have to be calculated during the extrapolation compared to a molecular dynamics simulation. While all pair interactions (inside the cutoff) have to be calculated in TI, only the interactions that change between the reference state and the extrapolated state are to be calculated in the extrapolations. The efficiency can be further increased by restricting the calculation to statistically independent configurations, thus re-

ducing the number of configurations by 1–2 orders of magnitude.

The method was benchmarked on a SGI O2 workstation with a R5000 processor at a 180-MHz clock speed. Benchmark V of the official GROMOS96 benchmarks (<http://igc.ethz.ch/gromos/benchmark.html>) is very similar to a typical system used here as a reference state. For the 1728 water molecules 150 s are required to simulate 100 steps using the standard GROMOS96. To simulate a 1.5 ns reference state with a time step of 2 fs this results in approximately 312.5 h of CPU time.

The resulting trajectory can be reduced in size by removing solvent molecules that are outside the cutoff of the extrapolated solute. An extrapolation using such a filtered trajectory in binary format on the same SGI O2 workstation takes approximately 0.5 h per compound. This has to be compared with a standard TI using a system of the same size as benchmark V. Using 25 λ points where at each λ point the system is equilibrated for 20 ps and averages are taken over another 50 ps, the overall simulated time amounts to 1.75 ns. Assuming again a 2 fs time step this results in approximately 365 h of CPU time per compound.

Conclusions

We described a method for estimating hydration free energies for small molecules from a *single* simulation. The method is based on the perturbation formula [eq. (3)] and uses so-called soft-core interactions [eqs. (4, 5)] as a *dummy* for the solute molecule.

The core height for the soft-core interaction that gave the best results was approximately 7 kJ/mol, which is roughly the average kinetic energy of a rigid water molecule. The widest sampling was achieved when the solvent molecules could on average just penetrate the cavity.

We showed that for small, apolar, rigid solute molecules the method is capable of yielding very accurate hydration free energies with errors below 1 kJ/mol. The treatment of flexible molecules can be included by sampling the internal degrees of freedom of the solute and correcting the averaging for the introduced intramolecular interaction. Statistics could be improved by additional sampling of center of mass positions and orientations of the solute molecules in the soft-core cavity. The method was applied to the estimation of solvation free energies in a highly polarizable environment:

water. We showed that using a 0.6 nm radius cavity the insertion of up to five atoms in a single step is possible. This cavity size was chosen simply as a demonstration of principle. To accommodate larger molecules a larger cavity would be required that could also be of arbitrary shape. This means that when applied to the modification of a reference molecule a very wide range of compounds can be encompassed in the approximation. The insertion of highly polar groups in a strongly polarizable medium using a nonpolar (hydrophobic) reference state is problematic. However, it does not represent any fundamental limitation of the approach, only that there is a need to develop alternative reference states that include configurations with some preorganization of the environment. We note that the choice of reference state (with a broad range of configurations) is of more importance in obtaining good accuracy than extending the length of a simulation with a not very appropriate reference state (which extends the sampling of nonrelevant configurations). As with particle insertion and all related approaches based on the thermodynamic perturbation formula, the method suffers from a lack of unambiguous convergence criteria. Nevertheless, the gain in efficiency over conventional free energy calculations based on using TI or thermodynamic perturbation with multiple intermediate states is potentially 2–3 orders of magnitude. Clearly this warrants both further investigation of possible improvements for polar solutes and application to systems of practical interest containing nonpolar solutes.

References

1. van Gunsteren, W. F. In *Computer Simulation of Biomolecular Systems, Theoretical and Experimental Applications*; van Gunsteren, W. F.; Weinert, P. K., Eds.; Escom Science Publishers: Leiden, The Netherlands, 1989; Vol. 1, p. 27.
2. Kirkwood, J. G. *J Chem Phys* 1935, 3, 300.
3. Levy, R. M.; Belhadj, M.; Kitchen, D. B. *J Phys Chem* 1991, 95, 3627.
4. King, G.; Barford, R. A. *J Phys Chem* 1993, 97, 8798.
5. Åqvist, J.; Medina, C.; Samuelsson, J.-E. *Protein Eng* 1994, 7, 385.
6. Smith, P. E.; van Gunsteren, W. F. *J Chem Phys* 1994, 100, 577.
7. Carlson, H. A.; Jorgensen, W. L. *J Phys Chem* 1995, 99, 1066.
8. Hummer, G.; Szabo, A. *J Chem Phys* 1996, 105, 2004.
9. Liu, H.; Mark, A. E.; van Gunsteren, W. F. *J Phys Chem* 1996, 100, 9485.
10. Zwanzig, R. W. *J Chem Phys* 1954, 22, 1420.
11. Radmer, R. J.; Kollman, P. A. *J Comput Chem* 1997, 18, 902.

12. Onsager, L. *J Chem Phys* 1936, 58, 1487.
13. Åqvist, J.; Hansson, T. *J Phys Chem* 1996, 100, 9512.
14. Matyushov, D. V.; Schmid, R. *J Chem Phys* 1996, 105, 4729.
15. Wood, R. H. *J Phys Chem* 1991, 95, 4838.
16. Mark, A. E.; van Gunsteren, W. F. In *New Perspectives in Drug Design; Proceedings of the 9th International Roundtable*, April 11–13, 1994, Turnberry, Scotland; Dean, P. M.; Jolles, G.; Newton, C. G., Eds.; Academic Press: London, 1995; Vol. 1, p. 185–200.
17. Widom, B. *J Chem Phys* 1963, 39, 2808.
18. Berendsen, H. J. C.; Postma, J. P. M.; van Gunsteren, W. F.; Hermans, J. In *Intermolecular Forces*; Pullman, B., Ed.; Reidel: Dordrecht, 1981; p. 331–342.
19. Ryckaert, J.-P.; Ciccotti, G.; Berendsen, H. J. C. *J Comput Phys* 1977, 23, 327.
20. Berendsen, H. J. C.; Postma, J. P. M.; van Gunsteren, W. F.; DiNola, A.; Haak, J. R. *J Chem Phys* 1984, 81, 3684.
21. Tironi, I. G.; Sperb, R.; Smith, P. E.; van Gunsteren, W. F. *J Chem Phys* 1995, 102, 5451.
22. van Gunsteren, W. F.; Billeter, S. R.; Eising, A. A.; Hünenberger, P. H.; Krüger, P.; Mark, A. E.; Scott, W. R. P.; Tironi, I. G. *Biomolecular Simulation: The GROMOS96 Manual and User Guide*, Vdf Hochschulverlag: Zürich, Switzerland, 1996.
23. Hansen, J. P.; McDonald, I. R. *Theory of Simple Liquids*; Academic Press: New York, 1986.
24. Wood, R. H.; Mühlbauer, W. C. F.; Thompson, P. T. *J Phys Chem* 1991, 95, 6670.
25. Torrie, G. M.; Valleau, J. P. *J Comput Phys* 1976, 23, 187.